Progress in Oceanography
June 2023, Volume 213, Pages 103002 (16p.)
https://doi.org/10.1016/j.pocean.2023.103002
https://archimer.ifremer.fr/doc/00823/93516/

Mechanisms underlying the epipelagic ecosystem response to ENSO in the equatorial Pacific ocean

Barrier Nicolas [1, *], Lengaigne Matthieu [1], Rault Jonathan [1], Person Renaud [2], Ethé Christian [3], Aumont Olivier [2], Maury Olivier [1]

[1] MARBEC, Univ. Montpellier, CNRS, Ifremer, IRD, Sète, France
[2] LOCEAN, IRD, France
[3] IPSL, CNRS, France

* Corresponding author : Nicolas Barrier, email address : nicolas.barrier@ird.fr

Abstract :

The El Niño/Southern Oscillation is known to strongly impact marine ecosystems and fisheries. In particular, El Niño years are characterized, among other things, by a decrease in tuna catches in the western Pacific and an increase in the central Pacific, whereas these catches accumulate in the far western Pacific during La Niña conditions. However, the processes driving this zonal shift in the tuna catch (changing habitat conditions, currents or food availability) remain unclear. Here, we use an hindcast simulation from the mechanistic ecosystem model APECOSM that reasonably reproduces the observed zonal shift of the epipelagic community in response to ENSO to understand the mechanisms underlying this shift.

Although the response of modeled epipelagic communities to El Niño is relatively similar for the different size classes studied, the processes responsible for these changes vary considerably by organism size. One of the major results of our analysis is the critical role of eastward passive transport by El Niño-related surface current anomaliesfor all size classes. While the effects of passive transport dominate the effects of growth and predation changes everywhere for large organisms, this is not the case for intermediate-sized organisms in the western Pacific, where the decrease in biomass is first explained by increased predation and then decreased foraging success. For small organisms, changes in growth rate induced by the influence of temperature on fish physiology is an important process that reinforces the biomass increase induced by passive horizontal transport in the eastern Pacific and the biomass decrease induced by increased predation by intermediate-sized organisms near the dateline. Finally, contrary to what is often assumed, our model shows that active habitat-based movements are not required to explain the westward biomass shifts that are observed during ENSO.

This study illustrates the relevance of using a mechanistic ecosystem model to disentangle the role of the different processes controlling biomass changes. It highlights the essential dynamic role of ocean currents in shaping the response of marine communities to climate variability and its interaction with biological (e.g. growth) and ecological (e.g. foraging and predation) processes, whose relative importance varies with organisms' size and contribute to modify the community structure.

Keywords : Fish, Biomass, ENSO, El Niño, La Niña, Ecosystem modelling, DEB, Advection, Growh, Predation, Equatorial Pacific, APECOSM, Epipelagic, Ecosystem, Habitat

1. Introduction

Understanding the impact of climate variability and change on marine ecosystems is key for the countries that border the tropical Pacific and exploit its marine resources. The marine ecosystems in the tropical Pacific Ocean indeed support a variety of small-scale artisanal fisheries that are essential for food security and livelihoods of most tropical Pacific islands and riparian countries (Batista et al., 2014). They also support domestic and Distant Water Fishing Nations (DWFN) large-scale oceanic fleets that are responsible for 60% of the world's tuna catches and contribute substantially to the income of most Pacific Island Countries and Territories, through domestic production and the purchase of fishing rights (just in the Western and Central Pacific, the value of the total tuna catch has consistently fluctuated between 4.5 and 7.5 billion dollars since 2007, Williams & Ruaia 2021). Skipjack (*Katsuwonus pelamis*), yellowfin (*Thunnus albacares*) and young bigeye (*Thunnus obesus*) tunas make up the bulk of purse seine catches that dominate tropical tuna fisheries (Allain et al., 2018). Their catches generally occur in the warm (above 26°C) surface waters of the western and the eastern Pacific where they live, reproduce and feed opportunistically on a wide range of small planktonic and nektonic epipelagic prey. Indeed, the prevailing trade wind conditions in the tropical Pacific leads to the accumulation of warm waters in the western Pacific that are favorable to tropical tuna. These winds also cause an upwelling of cold and rich waters along the equator throughout the central and eastern equatorial Pacific and induce the accumulation of epipelagic tuna prey that are part of trophic chains resulting from the equatorial upwelling. Smaller quantities of yellowfin and bigeye tuna as well as the temperate

albacore tuna (*Thunnus alalunga*) are also caught by industrial longliners in sub-equatorial and sub-tropical regions (Allain et al., 2018).

The climatological distribution of tropical tuna is strongly altered by the El Niño/Southern Oscillation (ENSO), the Earth's most energetic year-to-year climate event (Williams & Terawasi, 2014; Cai et al., 2021). ENSO indeed has a significant impact on the physical and biogeochemical properties of the tropical Pacific Ocean. An El Niño event (i.e. the warm phase of ENSO) is characterized by a deepening of the thermocline and nutricline in the central and eastern Pacific, which causes a warming of sea surface temperatures and a reduction of primary production in these regions, via a reduction of the upward vertical flux of nutrients and cold waters (e.g. Chavez et al., 1999; Murtugudde et al., 1999). In contrast, the western Pacific Ocean is experiencing opposite changes with a shoaling of the thermocline and nutricline, resulting in a slight cooling. Zonal eastward advection of warm nutrient-poor waters by anomalous eastward currents also contributes to the decrease of biological productivity in the central Pacific (e.g. Chavez et al., 1999; Picaut et al., 2001). La Niña (i.e. the cold ENSO phase) are generally considered as a mirror image of El Niño, despite some asymmetric features.

These changes in the physical and biogeochemical characteristics of the tropical Pacific Ocean during ENSO ultimately affect high trophic level organisms, including exploited fish populations, through changes in habitat conditions (oxygen, temperature, light penetration), currents and food abundance and availability (Bertrand et al., 2020). Tuna fisheries data indicate that purse seine catches in the western Pacific generally move eastward dur-

ing El Niño events and retract westward during La Niña events, in conjunction with the zonal migration of the warm pool (Lehodey et al., 1997). The strength of the vertical temperature gradients at the thermocline level also exerts a strong control on the vertical distribution of tunas (e.g. Schaefer & Fuller, 2002). It vertically compresses their thermal and feeding habitat in the western Pacific during El Niño, which increases the formations of dense schools (Maury, 2017) thus promoting their catchability by purse seine fisheries (Bertrand et al., 2002). ENSO not only impacts ecosystems through horizontal and vertical movements of fish populations, but can also affect the survival of larvae, whose variability propagates through the population structure and may be eventually be detected in the adult population some time later (Yen & Lu, 2016; Kim et al., 2015).

Most of the observational studies analyzing the influence of ENSO on Pacific marine ecosystems rely on tuna catch data, the variation of which is not only controlled by climate variability effects on population abundance and distribution but also by changes in fishing effort distribution, catchability and various dynamic processes internal to the ecosystem (Hobday & Evans, 2013). In addition, these fisheries observations are heterogeneous, limited to narrow and varying gear-specific depth ranges (for instance the 0-150m surface layer for purse seine data), focused on a few species and small size ranges, so that potential climate signals in these data are likely to be biased and distorted by other factors (Hobday & Evans, 2013).

In complement to using fisheries observations, several ecosystem models have been developed as part of the Fisheries and Marine Ecosystem Model Intercomparison Project (Fish-MIP, Tittensor et al., 2018) to characterize

and understand marine ecosystem responses to climate fluctuations. These models have been used primarily to project biomass changes in response to global warming, generally pointing to a global decline of marine biomass, more pronounced for higher trophic levels and tropical waters (Lotze et al., 2019; Tittensor et al., 2021). While these models are now commonly used to project future changes in biomass, they are much less used to analyze their response to past climate variability. This is however necessary because (1) a reliable representation of past variations in fish biomass would improve confidence in their future projections and (2) a better understanding of the processes responsible for past variability would provide keys to improving the models and better understanding of future changes. To our knowledge, only the SEAPODYM (Lehodey et al., 2008) ecosystem model has been specifically used to assess the ecosystem response to ENSO in the tropical Pacific, focusing on the spatial dynamics of the skipjack population (Lehodey, 2001). This model is able to reproduce the large-scale zonal migration of the skipjack tuna population in the equatorial Pacific in response to ENSO, which they attribute to ENSO-related changes in temperature, prey and oxygen concentrations that are driving active movements of skipjack tuna. Analysis of this model also suggests that El Niño not only drives an eastward tuna displacement but also promotes strong larval recruitment (Senina et al., 2008).

However, most ecosystem models have certain limitations that may restrict their ability to capture the full complexity of ENSO's impact on ecosystems. In particular, they generally simulate the marine ecosystem in two dimensions, despite the inherently three-dimensional nature of the impacts of

El Niño events on the physical and biogeochemical oceanic properties (shoaling/weakening of the thermocline and the relation with oxygen for instance; Leung et al., 2019). They also generally do not consider the effect of passive transport by ocean currents or active movements along environmental gradients and when they do, this transport is applied to only a limited number of size or age classes. Furthermore, they rarely simultaneously include the bottom-up and top-down effects of predation as well as the various metabolic processes (growth, reproduction, development, maintenance, mortality) that contribute to the transfer and dissipation of energy along food chains and cause temporal changes characteristic of environmental variability.

The objective of this paper is to revisit the question of ENSO impacts on tropical Pacific Ocean ecosystems using the mechanistic ecosystem model APECOSM (Maury, 2010), which doesn't suffer from the main limitations highlighted above (2D models, no passive or swimming movements for instance) and which considers explicitly the associated bio-ecological complexity. We focus our analysis on understanding the different bio-ecological processes by which ENSO influences the epipelagic community, which is the most intensively exploited pelagic community, especially by industrial purse seine fisheries targeting skipjack and yellowfin tunas. Overall, we show that the role of passive transport through El Niño related surface current anomalies is critical, not only for small organisms as usually assumed, but also for medium and large organisms. Furthermore, while passive transport effects dominate biomass changes for large organisms, we show that they can be amplified or offset for medium and small organisms by the interplay of bio-ecological processes such as temperature effects on growth, foraging success, and predatory

mortality, in ways that differ in the western and central Pacific. Contrary to what is often assumed (e.g. Lehodey 2001; Lehodey et al. 2020), our model shows that active habitat-based movements are not required to explain the westward biomass shifts that are observed during ENSO.

The document is organized as follows. Section 2) first describes the physical, biogeochemical and ecosystem models used in this study. Section 3 then assesses the ability of these models to reproduce the response to ENSO variability by comparing them to observations. Section 4 then investigates the dynamic and biological processes responsible for the modeled response of epipelagic fish biomass to El Niño events as a function of the size class. Finally, section 5 concludes this study by highlighting the main results, limitations and perspectives of this work.

2. Numerical models

Mechanistic ecosystem models such as APECOSM used here are valuable tools to understand the mechanisms that govern the variability of ocean ecosystems. They generally require physical and biogeochemical forcings (temperature, currents, oxygen, low-trophic levels concentration) as inputs. In the present study, the APECOSM model is forced by the outputs from a coupled physical and biogeochemical simulation, which is described in section 2.1. The ecosystem simulation is then discussed in section 2.2.

2.1. Physical and biogeochemical model

The three-dimensional physical and biogeochemical fields required to run APECOSM are extracted from an oceanic simulation performed with the physical ocean model NEMO (Nucleus for European Modelling of the Ocean,

Madec et al., 2019) coupled to the ocean biogeochemical model PISCES (Pelagic Interaction Scheme for Carbon and Ecosystem Studies, Aumont et al., 2015).

NEMO simulates the dynamics and thermodynamics of the physical ocean. Prognostic variables are the zonal and meridional velocity fields, a non-linear sea surface height, the conservative temperature and the absolute salinity, distributed on a three-dimensional Arakawa C-type grid. Density is computed from potential temperature, salinity and pressure using the IOC et al. (2010) equation of state. Vertical mixing is parameterized from a turbulence closure scheme based on a prognostic vertical turbulent kinetic equation, which has been shown to perform well in the tropics (Blanke & Delecluse, 1993). Lateral mixing acts along isopycnal surfaces, with a Laplacian operator and 200 $m^2 s^{-1}$ constant isopycnal diffusivity coefficient (Lengaigne et al., 2003). Shortwave fluxes penetrate into the ocean based on a single exponential profile (Paulson & Simpson, 1977) corresponding to oligotrophic water (attenuation depth of 23 m).

PISCES is a biogeochemical model of intermediate complexity with 24 prognostic variables designed for global ocean applications (Aumont et al., 2015). It simulates the biogeochemical cycles of oxygen, carbon and the main nutrients controlling phytoplankton growth (nitrate, ammonium, phosphate, silicic acid, and iron) and the lower-trophic level concentrations of marine ecosystems, distinguishing four plankton functional types based on size: two phytoplankton groups ("small phytoplankton" -e.g. nanophytoplankton- and "large phytoplankton" -e.g. diatoms-) and two zooplankton groups ("small zooplankton" -e.g. microzooplankton- and "large zooplankton" -

e.g. mesozooplankton-). It also includes small and large particulate organic matter.

The NEMO-PISCES simulation used in this study is deployed on the tripolar ORCA1 grid (Madec & Imbard, 1996), with a 1° nominal horizontal resolution and a refined 1/3° meridional resolution in the equatorial band. Its vertical resolution ranges from 1m at the surface to 100m at 1 kilometer depth and varies over time, following Levier et al. (2007). This simulation is forced over the 1958-2018 period with atmospheric inputs from the JRA atmospheric reanalysis (Kobayashi et al., 2015), which is representative of surface atmospheric variability observed over the historical period.

2.2. Marine ecosystem model

We use the Apex Predators Ecosystem Model (APECOSM, Maury et al., 2007; Maury, 2010) to simulate the energy transfer through marine ecosystems. APECOSM is a eulerian ecosystem model that represents the three-dimensional dynamics of size-structured pelagic populations and communities mechanistically. It integrates individual, population and community levels and includes the effects of life-history diversity with a trait-based approach (Maury & Poggiale, 2013). In APECOSM, energy uptake and utilization for individual growth, development, reproduction, somatic and maturity maintenance are modeled according to the Dynamic Energy Budget (DEB) theory (Koojman, 2010). The DEB theory is a comprehensive mechanistic theory of metabolism. It has been extensively tested empirically. In APECOSM, it allows the dynamics of the main components of metabolism and life history and their size, temperature and food dependence to be represented together. In addition to metabolism, APECOSM considers important ecological processes

such as opportunistic size-structured trophic interactions and competition for food, predatory, disease, ageing and starvation mortality, key physiological aspects such as vision and respiration, as well as essential processes such as three-dimensional passive transport by marine currents and active habitat-based movements (Faugeras & Maury, 2005), schooling and swarming (see Maury et al., 2007; Maury & Poggiale, 2013; Maury, 2017 for a detailed description of the model).

As discussed in Maury & Poggiale (2013), size-based predation implies that predation rates are controlled by the ratio of sizes between prey and predators (all organisms can be potentially predators and preys at the same time, depending on their relative size, cf. equation D1 of Maury & Poggiale (2013) for the detailed equation of the selectivity curve). Opportunistic predation implies that preys of a given weight are eaten in proportion to their selected available biomass relatively to the biomass of all possible preys available.

All the metabolic rates are temperature-dependent and corrected by an Arrhenius factor (Maury et al., 2007; Maury & Poggiale, 2013). While it can be prescribed in the model configuration, no preferred temperature range has been used in this study. Therefore, while temperature influences metabolism and swimming speed, its *horizontal gradient* does not influence the direction and magnitude of horizontal active swimming.

In APECOSM, the dynamics of communities is determined by integrating the core state equation below:

$$\partial_t \varepsilon = \underbrace{-\partial_w(\gamma\varepsilon) + \frac{\gamma}{w}\varepsilon}_{Growth} \quad \underbrace{-M\varepsilon}_{Mortalities} \quad \underbrace{-\overrightarrow{\nabla}.(\overrightarrow{V}\varepsilon)}_{3DAdv} \underbrace{+\overrightarrow{\nabla}.(D\overrightarrow{\nabla}\varepsilon)}_{3DDiff.} \tag{1}$$

where ε is the organisms' biomass density in the community, w their individual weight, γ is the growth rate, M represents the different mortality rates (computed using equation 12 of Maury & Poggiale 2013), V and D the sum of 3D passive and active velocities and diffusivity coefficients (computed following Faugeras & Maury 2005). The growth contribution is made of an advection (i.e. the biomass transfer along the size-spectrum, left-hand side) and a source term (i.e. biomass creation, right-hand side). Reproduction is considered through a Dirichlet boundary condition that injects the reproductive outputs from all mature organisms in w_0.

In APECOSM, the energy ingested by organisms fuels individual metabolism according to the DEB theory. Ingestion is proportional to a functional Holing type II response function that depends on the size-dependent visibility of prey, their aggregation in schools and temperature. This functional response can be written in a simplified way as follows:

$$f_{c,w} = \frac{P_{c,w}}{\frac{C_{c,w}A(T)}{h_c^{light}s_{c,w}(T)} + P_{c,w}} \tag{2}$$

with $P_{c,w}$ the prey biomass that is available to predator of community c (see Maury & Poggiale 2013 for details) and size w, $C_{c,w}$ the half-saturation constant, $A(T)$ the Arrhenius response of metabolism to temperature T, h_c^{light} the response of vision to ambient light and $s_{c,w}(T)$ the predator speed.

In the APECOSM model, oxygen concentration only modifies the hori-

zontal and vertical habitat of the different communities and size-classes and do not modify, in its current state, the biological parameters or the physiological rates. Considering the region of interest of the given study, this limitation has barely no consequence. Which would not be the case if analysing outputs within an Oxygen Minimum Zone (OMZ).

The APECOSM simulation used in this study is forced by three-dimensional temperature, horizontal current velocities, dissolved oxygen concentration, diatoms, mesozooplankton, microzooplankton and big particulate organic matter carbon concentrations (Aumont et al., 2015), photosynthetically active radiation (PAR) and dynamic layer thickness outputs from the NEMO-PISCES simulation (section 2.1). Nutrients concentrations simulated by NEMO/PISCES are not used as a forcing to Apecosm.

The APECOSM simulation runs with a daily time step for the biological processes, which is decomposed into a day/night cycle, the duration of which depends on latitude and day of the year (Forsythe et al., 1995). A sub time-stepping ($dt = 0.8h$) is used for horizontal advection and diffusion to ensure numerical stability.

The depth dimension is explicit, i.e. each biological variable (mortality, functional response) is computed in 3 dimensions (depth, latitude, longitude). The vertical distribution is thus determined from habitat functions that depend on the choice of the communities. In this study, three interactive communities are simulated:

- The epipelagic community, which includes the organisms that are feeding during the day near the surface such as yellowfin or skipjack tunas for example. Its vertical distribution is influenced by light and visible

food during daytime as well as temperature and oxygen during both day and night, while its functional response is influenced by light and temperature.

- The migratory mesopelagic community, which feeds in the surface layer at night and migrates to deeper waters during the day. Its vertical distribution is influenced by light and visible food during the night.

- The resident mesopelagic community, which remains at depth during both night and day. Its vertical distribution is influenced by light and visible food during the day.

To ensure that the size-spectrum is fully unfolded and a pseudo-steady state is achieved, the model was integrated successively over three 1958-2018 cycles. It was first initialized with an arbitrary small biomass value in each size-class and community and integrated from 1958 to 2018 (61 years). Then, the end of this first integration phase was used to run another cycle, which in turn was used to initialize the simulation analyzed in this study.

For each community, equation 1 is integrated over 100 logarithmically distributed size classes, ranging from $0.123cm$ to $196cm$. Since saving the outputs in 3D for the 3 communities and 100 size-classes is very costly, mortality rate, growth rate and functional response for each community and size are vertically averaged as follows:

$$F(y,x,c,w) = \frac{\sum_{z=0}^{H} F(z,y,x,c,w)B(z,y,x,c,w)}{\sum_{z=0}^{H} B(z,y,x,c,w)} \tag{3}$$

with x the longitude, y the latitude, z the depth, c the community, w the size-class, F the variable to consider (functional response, mortality rate,

growth rate) and B the 3D biomass (in $J.m^{-3}$).

In the remainder of the paper, the focus is solely put on the response of the epipelagic community; its near-surface location makes it more sensitive to ENSO variability (Le Mézo et al., 2016), it corresponds to organisms such as skipjack and yellowfin that are targeted by the industrial purse seine fleet, it accounts for the majority of tuna catches in the region, and have been reported to respond markedly to ENSO (Lehodey et al., 1997).

3. Evaluation of the modeled response to ENSO

Before analysing the main processes responsible for the modeled response of epipelagic communities to ENSO (next sections), we first assess the ability of the physical, biogeochemical and biological models that we use to reproduce ENSO-related fluctuations. Previous studies have already demonstrated the ability of NEMO-PISCES to reproduce many aspects of the physical (e.g., Vialard et al. 2001; Lengaigne et al. 2012; Drushka et al. 2015; Puy et al. 2019) and biogeochemical (e.g., Masotti et al. 2011; Gorgues et al. 2010; Martinez et al. 2020) response to ENSO in the tropical Pacific. In the following subsection, we briefly demonstrate the ability of our simulation to capture ENSO-related signals that are important to marine ecosystems, namely surface temperature (which modulates the functional response to prey as well as all the metabolic rates controlling growth, reproduction, development, maintenance and swimming speed in APECOSM), sea level anomalies (a proxy for thermocline depth, which modulates vertical habitats of epipelagic species), surface currents (which passively transport simulated biomass) and chlorophyll concentration anomalies (a proxy for primary production that fuels the

food chain).

3.1. Physical response

Figure 1a-c first assesses the ability of our simulation to reproduce the ENSO signature in sea surface temperature (SST). Figure 1a presents the temporal evolution of ENSO as observed and simulated by the physical model using the Oceanic Niño Index (hereafter ONI[2]), computed from a 3-month running mean of SST anomalies averaged over the Niño 3.4 region (5N-5S, 170W-120W). Over the entire period considered (1958-2018), the ONI index exceeds 2°C only on three occasions, corresponding to the three most intense El Niño events observed over the period considered (1982/83, 1997/98 and 2015/16). Other smaller El Niño events are also observed in 1986/87, 1991/92, 2002/03 and 2009/2010, with ONI values ranging between 1°C and 2°C. Major La Niña events are observed in 1970/71, 1973/74, 1988/89, 1999/2000, 2007/08 and 2010/11. This panel also reveals that the model is able to accurately simulate the timing and amplitude of ENSO events, as shown by the strong correlation (0.92) between observed and modeled ONI indices, significant at the 95% level of confidence (based on a Student t-test with an effective number of degrees of freedom that is corrected based on the 1 month-lag autocorrelation of each time-series, as reported in Bretherton et al., 1999). Despite this very good general agreement, the model tends to overestimate the amplitude of the strongest El Niño events.

Figure 1b-c then illustrates typical spatial SST patterns associated with ENSO for the observations (HadISST1, Rayner et al., 2003) and the model,

[2] https://www.cpc.ncep.noaa.gov/data/indices/oni.ascii.txt

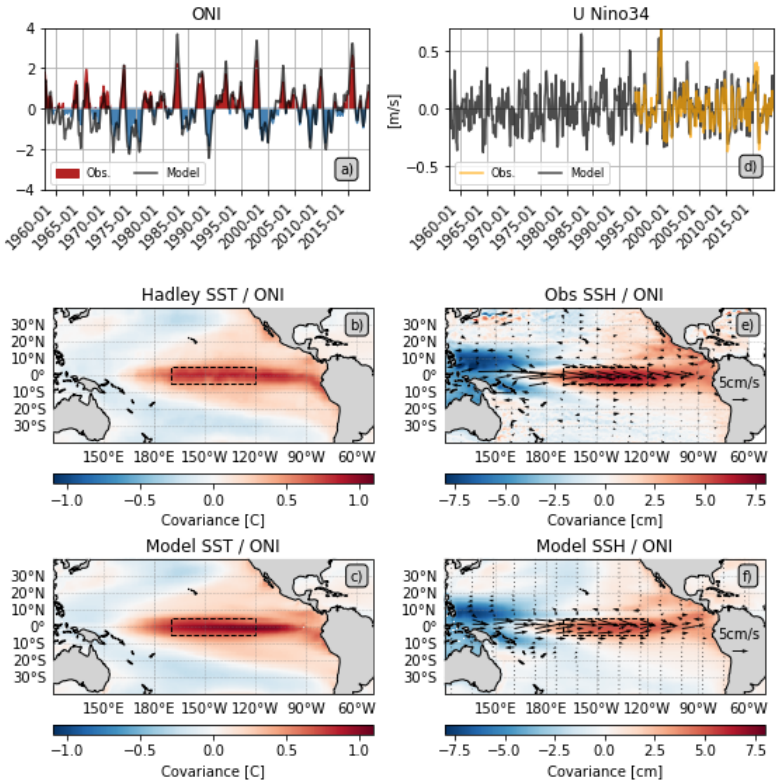

Figure 1: Time evolution of the ONI index for observations and model over the 1958-2018 period (a). ENSO-related SST patterns for observations (Rayner et al., 2003) (b) and model (c) derived from covariance maps of detrended monthly SST anomalies onto the ONI index over the 1958-2018 period. Time evolution of zonal surface current anomalies over the Niño34 region for observations over the 1993-2018 period (Rio et al., 2014) and model over the 1958-2018 period (d). ENSO-related sea-level and ocean current patterns for observations (e) and model (f) derived from covariance maps of detrended monthly sea-level and current anomalies onto the ONI index over the 1993-2018 period. The dashed box represents the Niño34 region used for averaging.

based on the covariance maps of detrended monthly SST anomalies onto the ONI index. The observed and modelled SST patterns are very similar and are characterized by warm SST anomalies (1°C) located in the central and eastern equatorial Pacific, flanked by the traditional horseshoe cooling pattern in the western Pacific that extends into the northern and southern subtropical Pacific.

ENSO-induced SST variations are known to be strongly related to variations in ocean currents and sea level (a proxy for thermocline depth), with SST signals largely driven by vertical displacement of the equatorial thermocline in response to equatorial wind variations. Figure 1d illustrates the temporal evolution of zonal current anomalies averaged over the Niño34 region for observations[3] (Rio et al., 2014) available from 1993 to present, and the model. The model faithfully reproduces the observed anomalies (significant correlation of 0.89), with eastward currents anomalies during El Niño events (reaching 0.7 m.s-1 at the peak of the 1982/83 and 1997/98 events) and westward currents anomalies during La Niña events. As shown in Figure 1e, these easterly current anomalies during El Niño are seen over the entire equatorial Pacific between 2N and 5S, a spatial structure well captured by the model (Figure 1f). With respect to sea-level, its ENSO related observational signature[4] (Figure 1e) is characterized by a shoaling of the thermocline in the western Pacific (negative sea level anomalies) and a deepening in the central and eastern Pacific (positive sea level anomalies), a signal that is physically consistent with the cooling observed in the west and the warming in the east

[3] https://doi.org/10.48670/moi-00050
[4] https://doi.org/10.48670/moi-00148

(Figure 1b). As shown in Figure 1f, the model captures this zonal sea-level tilt very accurately.

3.2. Biogeochemical response

Figure 2a-c assesses the ability of our simulation to capture ENSO-related variability of cholorophyll concentration. To this end, we compare simulated chlorophyll concentrations with multi-satellite monthly CHL-a estimates from the OceanColour-CCI V5 dataset[5] (Sathyendranath et al., 2019), available over the 1997-09/2018-12 period.

Figure 2a represents the temporal evolution of chlorophyll anomalies averaged over the equatorial Pacific for the model and observations. In agreement with past literature, El Niño events are associated with a decrease in chlorophyll all along the equator (Figure 2a) in response to the combined action of nutricline deepening in the eastern Pacific and eastward advection of nutrient-poor waters by anomalous eastward currents in the western and central Pacific. The reverse occurs during La Niña events. As a result, equatorial chlorophyll anomalies are strongly anti-correlated with variations in Niño34 SST (R=-0.74) and sea level (R=-0.78). The model faithfully reproduces these observed chlorophyll variations, with a correlation coefficient between the observed and simulated time series reaching 0.80 (significant at the 95% level of significance).

Figure 2b-c show typical spatial patterns of ENSO-associated surface chlorophyll anomalies for the observations and the model over their common period. In agreement with Figure 2a, El Niño causes a decrease in

[5] http://dx.doi.org/10.5285/1dbe7a109c0244aaad713e078fd3059a

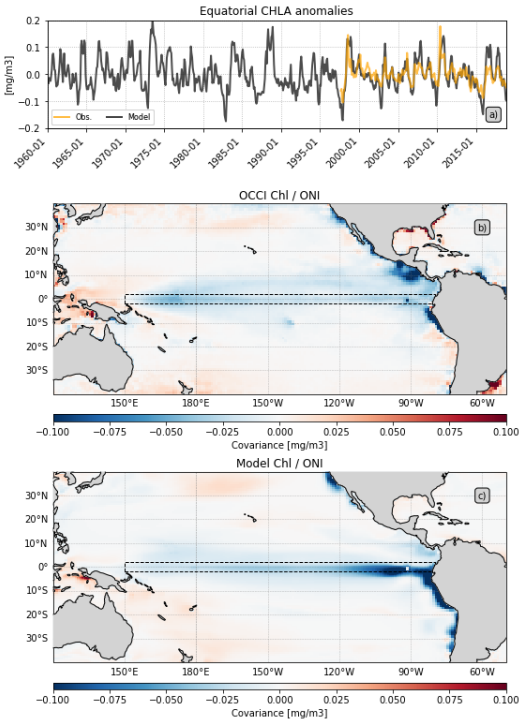

Figure 2: Time evolution of monthly surface chlorophyll anomalies in the equatorial Pacific for observations over the 1998-2018 period(yellow curve) and model over the 1960-2018 period (black curve) (a). Covariance between the chlorophyll anomalies and the ONI index over the 1998-2018 period for observations (b) and model (c). The dashed box represents the equatorial region used in the averaging.

chlorophyll concentration along the equator east of 150°E. Despite an overestimation of the modeled chlorophyll decrease in the eastern Pacific and an underestimation off Panama, the observations (upper panel) and the model (lower panel) show similar patterns. Note that recalculating the simulated spatial pattern over the entire modeled period (1958-2018) gives similar patterns (not shown).

3.3. Ecosystem response

In this section, we compare the evolution of the simulated epipelagic biomass to available observations in the equatorial Pacific. As mentioned in the introduction, the largest set of interannual observations of high trophic level marine organisms in the equatorial Pacific is based on tuna catches. Here we use monthly catches of skipjack and yellowfin tuna by purse seiners provided at 1° and 5° spatial resolution by the Western and Central Pacific Fisheries Commission (WCPFC) and processed by the French National Research Institute for Sustainable Development (IRD), as described in Taconet et al. (2018)[6]. We first extract skipjack and yellowfin purse-seine catches from the raw input file. We then discard observations with a temporal resolution greater than one month and data for which the geographical coordinates are not referenced in the database. The remaining observations are finally binned onto a regular $1° \times 1°$ grid. The final product consists of monthly maps of tuna catches covering the 1959-2018 period. However, due to the limited spatial coverage of the purse-seine fleets in the early part of the record, we only analyse this dataset from 1985 onwards. We compare catch observations to

[6] https://doi.org/10.5281/zenodo.1164128

the biomass of the epipelagic community integrated from 30cm to 70cm, the typical size range of skipjack and yellowfin tunas caught by purse seiners in this region. In making this comparison, it should be kept in mind that fishing data not only depend on the available fish biomass but are also influenced by both climate variability and the many socio-economic factors that control the dynamics and distribution of fishing effort (Hobday & Evans, 2013). Furthermore, although tuna represent the majority of epipelagic biomass in this size range in this region, the configuration of the model that we use here does not explicitly represent specific tuna species but generic oceanic communities such as the epipelagic community that we study here.

Figure 3a represents a longitude-time diagram of observed catches integrated between 10°N and 10°S over the 2008-2018 period. This panel highlights significant variations in the zonal extent of tuna catches in the equatorial Pacific. These catches are indeed confined to the west of the dateline during certain periods such as in 2008 and 2011, when La Niña conditions prevail over the Pacific. In contrast, they extend eastward into the central Pacific for other periods such as 2009-2010 and 2014-2016 that are characterized by El Niño conditions. Despite their different nature, the zonal extension of the modeled biomass compares surprisingly well with that of tuna catches over the recent period: La Niña events of 2008 and 2011 are indeed characterized by a westward retraction of the epipelagic biomass, while El Niño periods of 2009-2010 and 2014-2016 are characterized by a clear eastward extension of the epipelagic biomass.

Figure 3b-c show the differences in observed catches and simulated biomass between an El Niño (2009-10/2010-03, 2014-10/2015-03, 2015-10/2016-03)

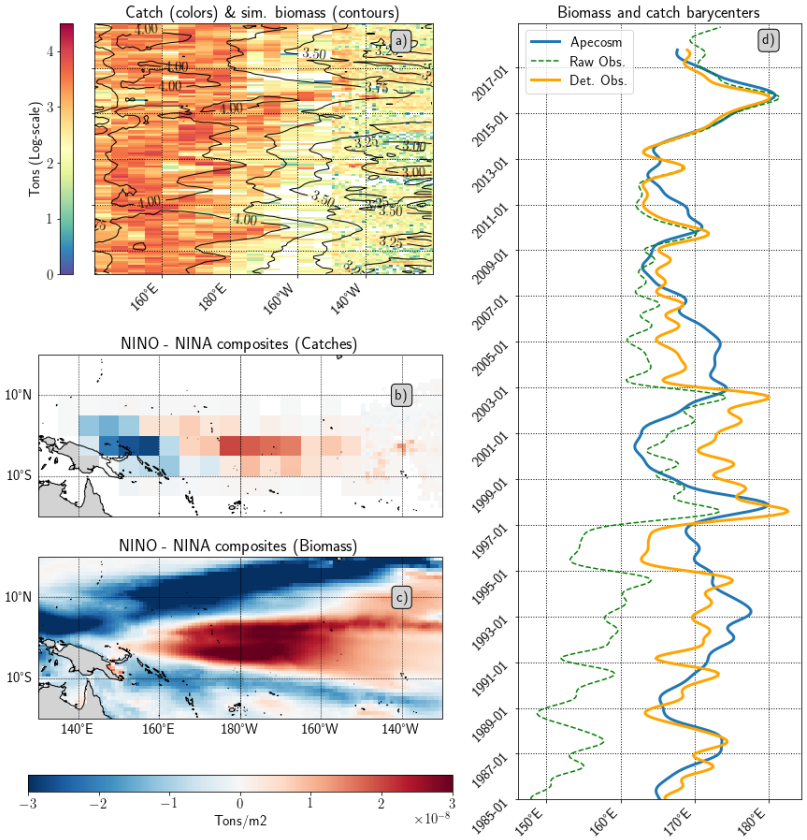

Figure 3: Time-longitude diagram of observed catches (colors, log-scale in Tons) and simulated epipelagic biomass (contours, log-scale in Tons) cumulated between 10°N and 10°S (a). Difference between El Niño and La Niña composites over the 2007-2018 period for observed catches (b) and simulated epipelagic biomass (c). Temporal evolution of the barycenters' longitudes of simulated epipelagic biomass (thick blue line) and observed catches (thin dashed-dotted green line) over the 1985-2018 period. The detrended catch barycenter is also shown (thick orange line) (d). Panels (a) and (d) are positionned so that their temporal axes are aligned. All panels have different x-axis.

and a La Niña composite (2007-10/2008-03, 2008-10/2009-03, 2010-10/2011-03, 2011-10/2012-03). Consistent with Figure 3a, it illustrates the typical east-west shift pattern that is associated with ENSO in the recent period. Observed catches are greater in the central and eastern Pacific and lower in the Western Pacific under El Niño conditions compared to La Niña conditions, corresponding to an eastward shift of the epipelagic biomass. Observed catches and simulated biomass composites show similar patterns, although slightly shifted westward in the model.

Figure 3d then assesses the agreement between the observations and the model over a longer period. It shows the temporal evolution of the barycenters' longitudes of observed tuna catches and modeled biomass over the 1985-2018 period, smoothed by a Gaussian filter ($\sigma = 3.5$ and truncation above 4σ). Consistently with the good agreement between model and observations presented in Figure 3a, the evolution of the model barycenter is very consistent with that of observations over the last decade (2008-2018), with a correlation of 0.88 between the two time series. This is particularly the case for the 2014-2016 El Niño sequence, where both model and observations indicate an eastward shift in the data barycenter from 160°E in early 2014 to 180°W in early 2016, before retracting westward after that date. Looking at the observations over the entire 1985-2018 period, the most striking feature is a gradual eastward shift in the location of the catches barycenter, from 155°E in the 80's to 170°E in the last decade. This trend is consistent with a global expansion of the industrial purse seine tuna fleet distribution over the last decades (Coulter et al., 2020).

Industrial tuna fisheries have indeed expanded considerably since the

1950s (e.g. Tickler et al. 2018; FAO 2022). This growth in production means and catches, accompanied by a considerable spatial extension, in particular due to the increase in the range of fishing vessels, is well documented on a global scale (e.g.: Fonteneau 1998) and in the western Pacific (Lodge, 1998; Williams & Ruaia, 2021) where it has notably translated into a progressive westward extension of the fishing areas of the purse seiners (Fonteneau, 1998). In order to take into account this geographical expansion when comparing the fisheries data with the model outputs over the long period, the observed time series has been detrended. The model and detrended observations show a reasonable match over the entire period, with a correlation of 0.45. The strong correlation coefficient of the ONI timeseries with the model biomass barycenter (0.74) as well as with the observed catches barycenter (0.52) further highlights the control exerted by ENSO in both observations and model, particularly during the 1986/87, 1997/98 or 2001/02 El Niño events, when observed catches shift eastward. While observations and the model generally shows a westward shift during La Niña conditions and an eastward shift during El Niño conditions, these time series deviate from each other during specific periods, such as the strong La Niña of 1999/2000, which is characterized by a stronger westward retraction in the model or during the warm years of 2003-2005 with the barycenter of observed catches shifting westward relative to that of the modeled biomass.

In summary, the analyses presented above illustrate the ability of the various model components to satisfactorily reproduce the physical, biogeochemical and ecosystem response to ENSO. In particular, the ecosystem model is able to simulate zonal shifts of the large organisms of the epipelagic com-

munity in response to ENSO in a manner similar to that observed for tuna catches. This agreement provides support for using our ecosystem simulation to study the processes responsible for the epipelagic community response to ENSO. In what follows, our results are detailed for three selected size classes: small epipelagic organisms (3 cm), intermediate sizes (20 cm), and large individuals (90 cm). The latter two are representative of the lower and upper limits of the size range of the tunas exploited by purse seiners in the region.

4. Response of the epipelagic community to extreme El Niño events

This section focuses on describing the simulated size-dependent response of the epipelagic community to ENSO and understanding the mechanisms responsible for this response. Here, we will specifically study the epipelagic community response to the three strongest El Niño events over the historical period, namely those of 1982/83, 1997/98 and 2015/16 (Santoso et al., 2017). During these events, the central and eastern Pacific warmed by more than 2°C (Figure 1a), moving the warm waters and associated atmospheric convection from the west to the central and eastern Pacific. The atmospheric signature of these El Niño has had dramatic climatic consequences, including droughts and forest fires in countries bordering the western Pacific, but also torrential rains and floods along the south American coast (Cai et al., 2020). Their oceanic signature also had major impacts on marine ecosystems and biodiversity, leading to significant disruptions in marine life and seabird populations (Valle et al., 1987), promoting large-scale marine heatwaves (Holbrook et al., 2020) and coral bleaching (Claar et al., 2018). The ocean response during each of these three extreme events has been exten-

sively described and analyzed in terms of physics (e.g. Philander & Seigel, 1985; Lengaigne et al., 2002; Puy et al., 2019), biogeochemistry (e.g. Barber & Chavez, 1983; Chavez et al., 1999; Stramma et al., 2016) and marine ecosystems (Glynn, 1988; Glynn et al., 2001; Eakin et al., 2019).

To isolate the generic response of epipelagic organisms to extreme El Niño events, independent of the intrinsic characteristics of each event, we perform a composite analysis of these three extreme events, averaging monthly anomalies of temperature, ocean velocity, low trophic level (LTL, i.e. phyto and zooplankton, particulate organanic matter) concentrations and biomass of the epipelagic community over the 1982-1983, 1997-1998 and 2015-2016 periods. These extreme El Niño events are also followed by La Niña conditions the following year (more intense in the case of the 1997/98 event), which also allows for a discussion of the epipelagic community response mechanisms to La Niña events. Although the temporal evolution and amplitude of the processes discussed below vary slightly between events, the relative importance of the processes discussed in our composite analysis remains qualitatively similar when these three extreme events are analyzed individually (not shown).

4.1. Model response from physics to ecosystems

As major environmental drivers of the epipelagic biomass variability, Figure 4a-c first depicts the temporal evolution of monthly equatorial anomalies in upper ocean temperatures, LTL concentration and zonal currents during and after extreme El Niño events, in the form of equatorial time-longitude diagrams, with the January month preceding the onset of the El Niño event as origin of time. The warming signal associated with El Niño initiates in the central equatorial Pacific in early spring, then spreads rapidly to the

eastern Pacific, intensifies during the summer and fall, peaks at the end of the calendar year, and finally declines rapidly and transitions to La Niña conditions the following spring (from April-y1, Figure 4a). The development phase of El Niño is also characterized by strong eastward surface currents anomalies in the western and central Pacific (Figure 4b) induced by anomalous westerly winds, promoting warming of the central Pacific and eastward movement of the warm-pool toward the eastern equatorial Pacific. These current anomalies reverse at the peak of El Niño and during La Niña. The simulated plankton concentration anomalies largely mirror those of temperature, with a sharp decrease during El Niño and an increase during La Niña (Figure 4.c).

A similar analysis is then performed for epipelagic biomass for the three selected size classes (Figure 4d-e-f). Their responses to El Niño share common characteristics: positive biomass anomalies appear near the dateline early in the calendar year and propagate eastward toward the central Pacific until late spring (May/June-y0). These positive biomass anomalies in the central Pacific re-intensify in fall and then rapidly disappear in winter. They are also accompanied by a decrease in biomass in the western Pacific from the beginning of the El Niño year. These negative anomalies persist after the El Niño peak and during the subsequent La Niña event but remain largely confined to the western Pacific. Despite similar behaviour, however, the response of the three size classes show some significant differences, including a westward shift in response as size class increases.

Figure 5 shows how these surface ENSO-related signals propagate in depth by providing climatological equatorial profiles, computed over the full

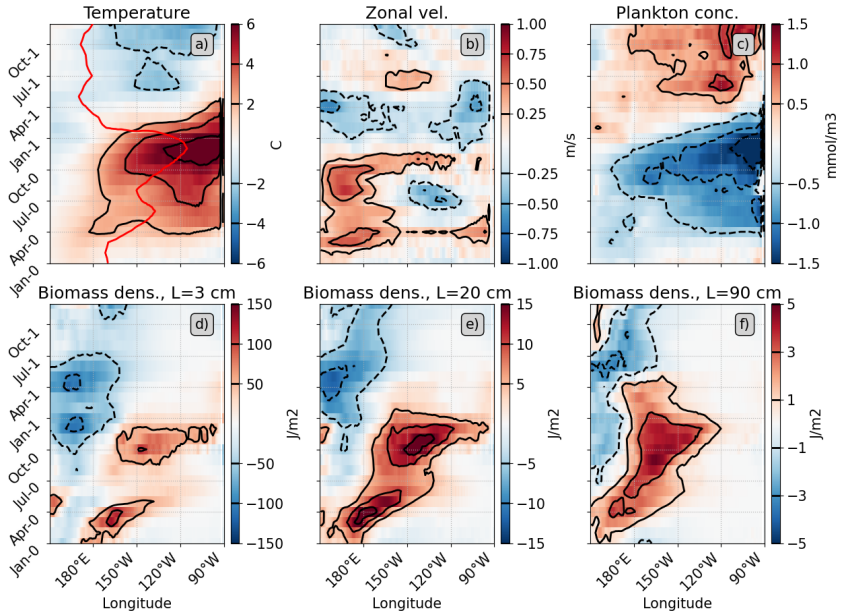

Figure 4: Time-longitude diagrams in the equatorial Pacific of surface temperatures (in °C) (a), zonal velocity (in m/s, positive eastward) (b), low-trophic level concentrations (in mmol/m3) (c) and fish biomass anomalies (in J/m2) associated with extreme El Niño events composite (3cm, 20cm and 90 cm in d, e, f, respectively). The eastern location of the warm pool (28° isotherm) is shown in red in (a).

simulated period (1958 to 2018, therefore including neutral, El Niño and La Niña conditions) of temperatures, zonal velocities, low-trophic level concentrations and epipelagic daytime biomass for the three size classes, as well as their boreal winter anomalies for extreme El Niño composites. The climatological temperature profile indicates that the thermocline is deep in the western Pacific and shallow in the east, and flattens during El Niño, resulting in warming in the east and cooling in the west (Figure 5a). The Equatorial Undercurrent also weakens strongly during El Niño, while strong positive (i.e. eastward) current anomalies occur near the surface (Figure 5b). Low trophic level biomass, which is maximal in the upper 50m of the eastern Pacific, decrease during El Niño, due to the flattening of the thermocline, which reduces the nutrient supply in the surface layers (Figure 5c). Regarding the vertical extent of the epipelagic community, the climatological biomass for the three classes in the western Pacific extends from the surface to $100m$ in the western Pacific and decreases during El Niño events. However, this decrease is not homogeneous along the vertical, with strong positive anomalies appearing around 40m in the west for intermediate and large sizes (Figure 5d-e-f). These are induced by a narrowing of the vertical habitat, due to the shallowing of the thermocline.

4.2. Processes driving the epipelagic upper-ocean response

The contribution of the different processes responsible for the epipelagic response to El Niño (Figure 4d-e-f) is now assessed by performing the same equatorial time-longitude diagrams for the main tendency terms (right members of equation 1) and their temporal integral, which represents their contribution to the total biomass change (as done in Guiet et al. 2022 to seperate

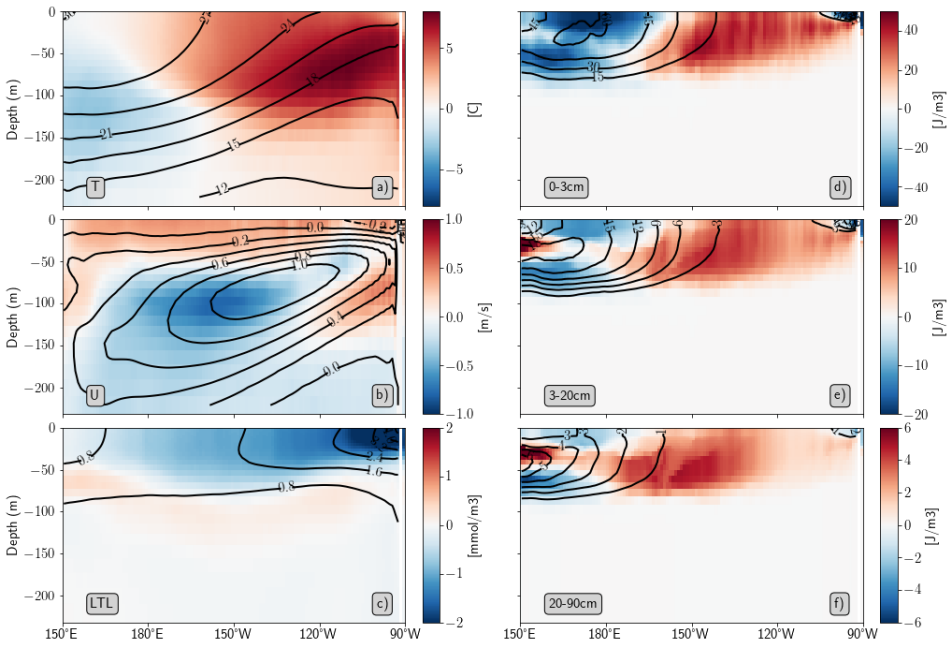

Figure 5: Pacific equatorial profiles of temperature (a), zonal velocity (b), low-trophic level concentration (c) and fish biomass (d for small, e for intermediate and f for large sizes). Climatological mean values over the full period (1958 to 2018, therefore including neutral, El Niño and La Niña conditions) are represented as black contour lines and El Niño composite anomalies are represented in colors.

passive advection and active swimming). We also analyze key parameters of the biological response to changing environmental conditions, namely growth rate (γ in equation 1), functional response (equation 2) and predation mortality rates (M in equation 1). Because the relative importance of each of these processes varies among size classes, these analyses are discussed separately for each size class.

Figure 6 provides a synthesis of the respective contributions of biological (i.e. the combined action of growth and predation) and physical (i.e. the combined action of advection and diffusion) processes on the epipelagic biomass response to ENSO for each of the three size classes. One inference that can be drawn is that the relative importance of biological processes decreases as fish size increases for two reasons. First, predation is size-based in the APECOSM model, resulting in high predation pressure on small organisms, which decreases with size since larger organisms have fewer predators in the model. Second, growth includes a flux term and a source term (see equation 1) that are both dependent on temperature. The source term controls biomass production and varies as γ/w, which scales linearly with $w^{-\frac{1}{3}}$ and thus decreases strongly with size.

The decrease of the small and intermediate size biomass in the western Pacific is thus primarily the result of biological processes. In the central and eastern Pacific, the combined action of dynamic and biological processes accounts for the increase in biomass during El Niño (Figure 6a-f) while these processes largely offset each other when the equatorial Pacific reverses to La Niña conditions, resulting in small changes in biomass in this region. For the largest size class, physical processes (Figure 6i) explain most of the

biomass changes (Figure 6g), with biological processes being negligible (Figure 6h).

The action of physical processes on biomass evolution is simple. It results from the transport of biomass from the western to the central Pacific in response to the strong eastward currents anomalies that occur during extreme El Niño conditions. It is experienced in a similar way by all size organisms, since the ocean current anomalies during El Niño (up to $0.6 m.s^{-1}$, see Figure 4c) dominate the volitional (i.e. swimming) velocity anomalies by a factor of $\approx$ 1000 for small sizes, 20 for intermediate sizes and 3 for large sizes (not shown).

The significant and sometimes dominant contribution of biological processes for small and medium size classes, however, is more difficult to understand intuitively because it results from the combined action of predation mortality and growth. Therefore, we further detail the respective contribution of predation and growth and their driving factors for small and medium size classes on Figure 7 and Figure 8 respectively.

For small size classes (3cm), the effects of predation mortality balance the effects of growth (Figure 7b-c), resulting in a net effect of biological processes that is much smaller than the effect of each biological process considered in isolation (Figure 7a). Growth leads to an increase in biomass at the onset of El Niño in the central Pacific (between dateline and 150°W), that spreads eastward to its peak. These positive biomass anomalies then decrease slightly during the following La Niña conditions (Figure 7b).

Figure 7e shows the functional response, which controls the predation swimming speed (that is proportional to the functional response's gradient),

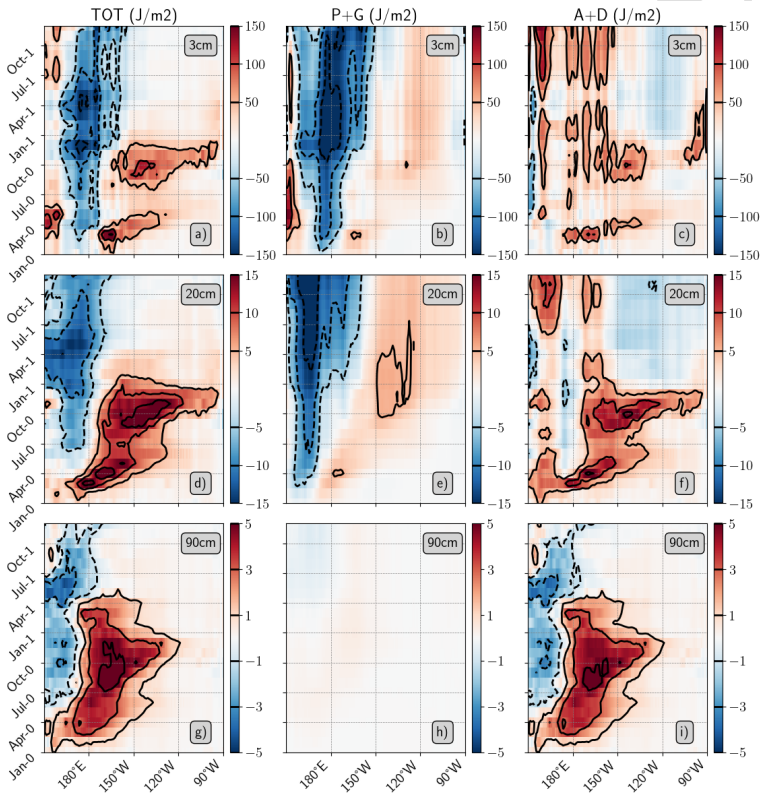

Figure 6: Time-longitude diagrams in the equatorial Pacific of total (left), biologically (middle, predation plus growth terms) and physically (right, advection plus diffusion) induced interannual variations in fish biomass (in $J.m^{-2}$) associated with extreme El Niño events composites for small (top), intermediate (middle) and large (bottom) sizes.

the vertical distribution and swarming level of epipelagic fish, which in turn control their availability to predators. Despite its importance in controlling growth and reproduction, our analysis indicates that the decrease in functional response is not the primary driver of biomass changes, since negative functional response anomalies are associated with positive biomass anomalies.

Instead, the increase in growth rate east of the dateline during El Niño closely follows the evolution of the anomalous warming (Figure 7e), suggesting that changes in growth rate are largely driven by the influence of temperature on fish physiology. In contrast to the central and eastern Pacific, the growth rate decreases in the western Pacific as it cools from July of the El Niño year, contributing to a decrease in biomass. Although these growth rate negative anomalies in the western Pacific are smaller than the positive ones in the eastern part, their impact on the biomass, which is proportional to the biomass itself (cf. equation 1) is greater since biomass levels are ten times larger in the west than in the east (see black contours in Figure 10).

As mentioned previously, predation-induced changes in biomass are largely opposite to growth-induced changes (Figure 7b-c). Predation-induced changes decrease biomass in the central and eastern Pacific and increase biomass in the far western Pacific (Figure 7c), closely following the changes in biomass of intermediate size predators (Figure 7f). Despite their opposite effect on biomass, growth effects generally slightly dominate those of predation, explaining most of the decrease in small size classes in the western Pacific during El Niño and the subsequent La Niña, and reinforcing the biomass increase in

the central Pacific induced by dynamic processes during El Niño. An exception is the very early decrease in biomass simulated near the dateline from February of the El Niño year, which is not driven by growth rate changes (Figure 7b) but rather by increased predation by intermediate size organisms at the El Niño onset (Figure 8c,f).

The growth and predation induced biomass changes for the intermediate size classes are similar to those simulated for small size classes (Figure 8): they are opposite and of the same order of magnitude, with growth effects generally dominating predation effects. Growth increases fish biomass in the central Pacific from the onset to the peak of El Niño. However, the influence of temperature on fish physiology is no longer the dominant factor of biologically induced biomass changes for intermediate size organisms as it was for small organisms. In contrast to small size classes, changes in growth rate largely reflect changes in functional response, which is increasing in the central Pacific due to both warmer waters (increased swimming speed controlling the attack rate parameter in the functional response) and increased food availability (due to the increased biomass of small organisms), both of which contribute to increase the biomass of intermediate size organisms in the central Pacific. In the western Pacific, the growth rate decreases only very modestly (Figure 8b) but, as seen for small size classes, this translates into a large reduction of growth-induced biomass from October onwards since its effect is proportional to biomass, which is ten times larger in the western than in the eastern Pacific (Figure 10). On the other hand, predation generally mitigates the effects of growth, reducing biomass in the central Pacific through increased predation by large size classes there and increasing biomass

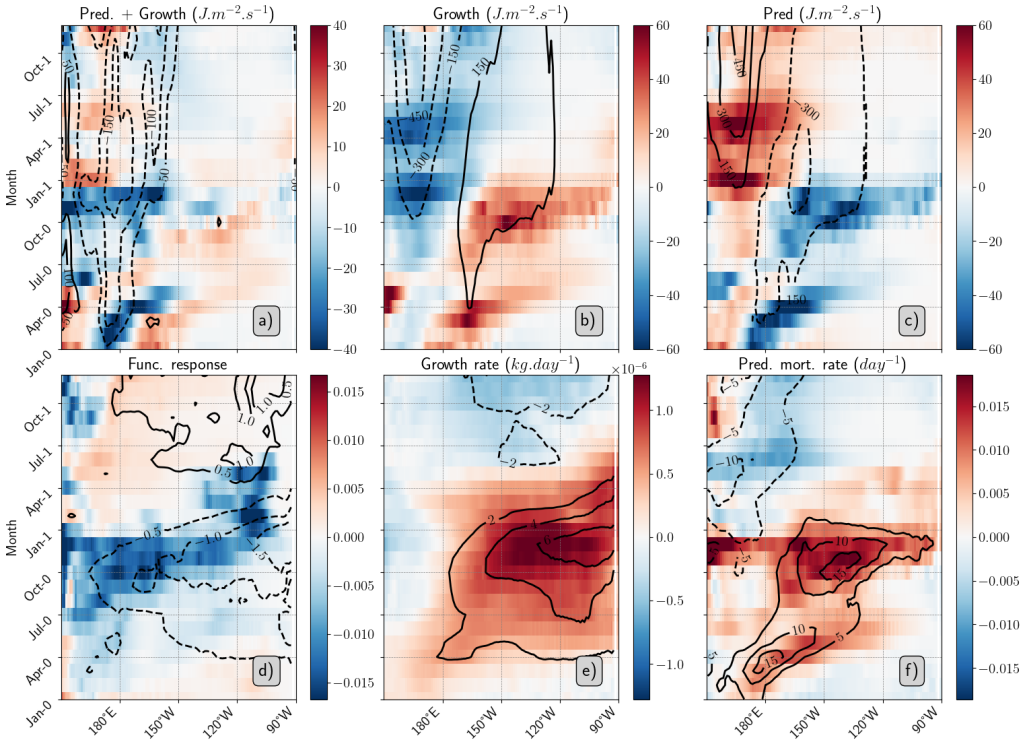

Figure 7: Time-longitude diagrams in the equatorial Pacific of interannual anomalies of small sizes biomass trends ($J.m^{-2}.s^{-1}$; in colors) and time-integrated trends ($J.m^{-2}$; in contours) associated with extreme El Niño events composite for predation plus growth (a), growth (b) and predation (c). Same as (a-c) but for interannual anomalies of the functional response (no unit; in colors) and planktonic prey biomass density ($mmol.m^{-3}$; in contours) (d), growth rate ($kg.day^{-1}$; in colors) and temperature (°C; in contours) (e) and predation mortality rate (day^{-1}; in colors) and intermediate size biomass ($J.m^{-2}$; in contour) (f).

in the western Pacific during the subsequent La Niña through reduced predation. This evolution largely resembles those obtained for small sizes, albeit with a modest westward shift. The changes induced by the combination of these two processes are generally dominated by growth, except in the western Pacific during El Niño development where the decrease in biomass from February onwards is due to increased predation by large organisms. As for small sizes, the decrease in biomass in the western Pacific during El Niño and the subsequent La Niña are initially due to increased predation followed by a reduction in growth, while dynamicrocesses dominate the biomass increase east of the dateline with a smaller contribution from growth.

Figure 9 provides a brief summary of the different processes involved in the epipelagic response to interannual ENSO variability that has been discussed in this section.

4.3. Generalization

All the analyses presented above focused on the equatorial Pacific, where ENSO physical and biogeochemical signatures are the strongest. To ascertain the response of off equatorial regions to ENSO, Figure 10 further provides maps of climatological epipelagic biomass for the three size classes as well as their boreal winter anomalies for extreme El Niño composites. On average, epipelagic fish biomass is largest both sides of the equator and in the equatorial western Pacific (Figure 10a-b-c), while smaller biomasses are found in the eastern Pacific. In agreement with the equatorial analyses provided on Figure 4, Figure 10a indicates that during El Niño, small epipelagic fish biomass increases in the equatorial eastern Pacific and decreases in the western Pacific. In addition, Figure 10a reveals that this biomass also decreases

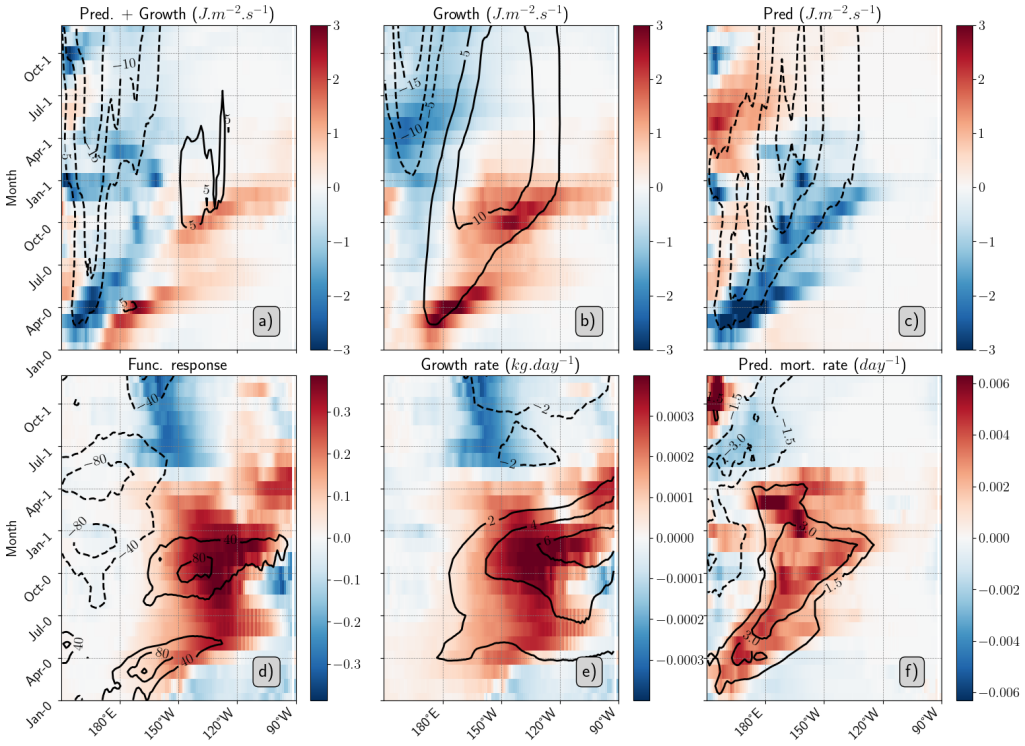

Figure 8: Time-longitude diagrams in the equatorial Pacific of interannual anomalies of intermediate sizes biomass trends ($J.m^{-2}.s^{-1}$; in colors) and time-integrated trends ($J.m^{-2}$; in contours) associated with extreme El Niño events composite for predation plus growth (a), growth (b) and predation (c). Same as (a-c) but for interannual anomalies of the functional response (no unit; in colors) and small prey biomass density ($J.m^{-2}$; in contours) (d), growth rate ($kg.day^{-1}$; in colors) and temperature (°C; in contours) (e) and predation mortality rate (day^{-1}; in colors) and large size biomass ($J.m^{-2}$; in contour) (f).

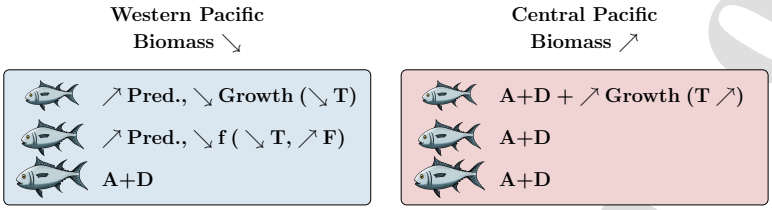

Figure 9: Summary of the processes involved in the response of epipelagic biomass to El Niño conditions. *Pred.* is predation, T is temperature, $A + D$ is advection/diffusion, f is the functional response and F is food concentration.

both sides of the equator, further highlighting that the biomass does not only shift eastward during El Niño but also equatorward. As size increases, positive anomalies associated with El Niño conditions expand westward and poleward while negative anomalies weaken and expand equatorward.

To insure that the biomass response described for extreme El Niño events is representative of ENSO variability in general, Figure 10d-e-f shows the covariance maps computed between the monthly ONI index and the detrended fish biomass anomalies for the three size classes over the 1958-2018 period. This analysis reveals that the patterns in extreme El Niño composites are very similar to covariance analyses, although amplitudes are about four times larger for extreme events. This difference in amplitude is related to the fact that the covariance analysis also includes weaker El Niño events (such as the 1986, 1991, 1994, 2002, 2004 and 2009 events) as well as La Niña events, which are known to have weaker physical and biogeochemical signatures. Nevertheless, the very good match between the covariance maps and the extreme El Niño composites indicates that the biomass response and related mechanisms discussed above for the three major El Niño events are also

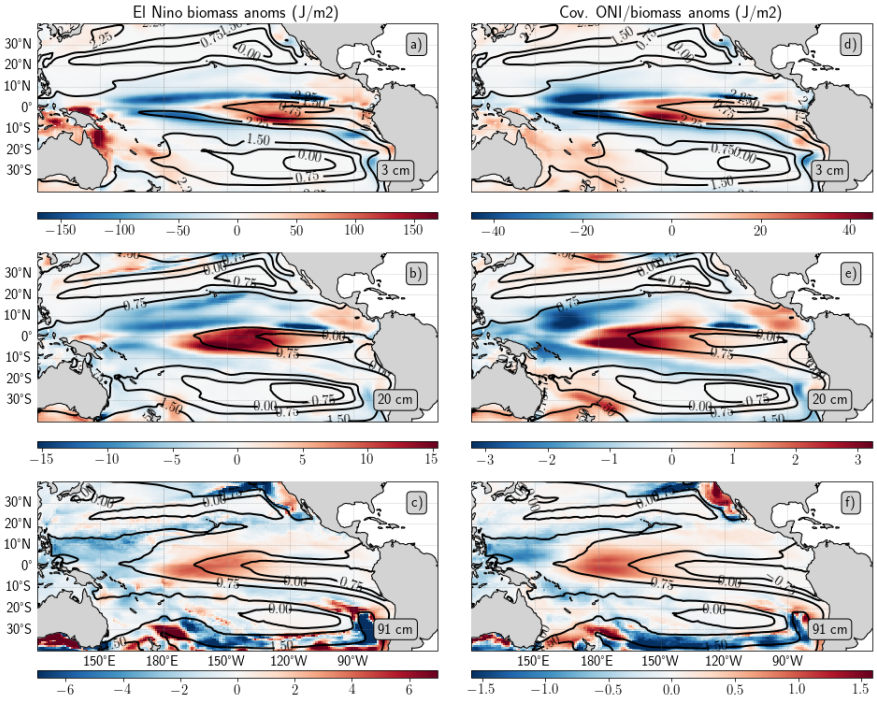

Figure 10: Maps of boreal winter (DJF) biomass anomalies for extreme El Niño events composites (left column) and covariance of fish biomass anomalies with the ONI index (right column) for small (upper line), intermediate (middle line) and large sizes (lower line). Black contours correspond to the climatological biomass density distribution (log-scale).

representative of other ENSO events.

5. Conclusion

5.1. Summary

ENSO, the most energetic interannual climate mode on a global scale, is known to strongly impact marine ecosystems through changes in habitat conditions (oxygen, temperature, light penetration), currents and food availability. In particular, tuna catch data point to a shift of epipelagic biomass from the equatorial western to the central Pacific in response to El Niño and an accumulation of the biomass in the extreme western equatorial Pacific in response to La Niña. These indirect and heterogeneous data, which do not solely reflect changes in fish populations, are insufficient to address address the mechanisms responsible for these changes. Here, we use a simulation from a mechanistic ecosystem model that captures the zonal shift of the epipelagic community in response to ENSO.Model results are similar to the response of tuna catches and allow, through the analysis of the tendency terms of biomass changes, us to unravel underlying mechanisms.

Despite a relatively similar modeled response of epipelagic communities to El Niño among different size classes, characterized by a decrease in biomass in the western Pacific and an increase in the central Pacific, our analyses reveal that the processes responsible for these changes vary considerably by size. For large organisms, eastward passive transport by El Niño related eastward surface currents anomalies is largely responsible for the movement of organisms from the western to the central Pacific and dominates the effects of growth and predation, which are structurally weaker for large organisms.

For intermediate-sized organisms, while the increase in biomass in the central Pacific is also largely explained by eastward advection by zonal currents anomalies, the decrease in biomass in the western Pacific is explained initially by increased predation by large organisms, and then by reduced growth due to a decrease in the functional response related to both colder waters and decreased food availability. For small organisms, changes in growth rate induced by the influence of temperature on fish physiology are an important process, reinforcing the increase in biomass induced by passive horizontal transport in the eastern Pacific and the decrease in biomass induced by increased predation by intermediate organisms near the dateline.

5.2. Discussion

Previous studies (e.g. Lehodey et al., 1997; Lehodey, 2001) have attributed the eastward biomass shift of skipjack tuna during El Niño to active swimming to track the eastward migration of favorable warm waters. Here we show that such a biomass shift can be realistically simulated without the need to specify temperature preferences that would lead to active movements of the tuna towards the most favorable waters. Passive horizontal transport by ENSO-related currents is indeed sufficient in our simulations to explain the eastward movement of tunas. Our study highlights that it is therefore essential that marine ecosystem models account for the dynamic role of ocean currents in shaping the spatial distribution of marine communities and their response to climate variability.

Our analysis demonstrates the added value of using a mechanistic ecosystem model to disentangle the role of the different processes controlling biomass changes and understand their interactions. The analysis of biomass tendency

terms is a particularly powerful tool to isolate the effects of dynamic processes (passive transport by currents) from those of biological processes (growth, reproduction and predation in particular), and understand how these different processes change with environmental conditions and with organism size. Thus, the mechanistic foundations of the APECOSM model, which is based on the DEB theory, are particularly well suited to an in-depth analysis of the processes involved.

While La Niña has long been largely considered a mirror image of El Niño, the study of asymmetries between these two phases of ENSO has recently become an important research topic (e.g., An et al. 2020). This interest is firstly driven by an amplitude asymmetry, where the most intense El Niño events reach much larger amplitudes than the most intense La Niña events, but also by a spatial structure asymmetry, where La Niña SST anomalies are shifted westward and have a wider meridional extent compared to that of El Niño (e.g. Takahashi et al. 2011). In this study, we focused primarily on the ecosystem response to extreme El Niño events because of their dramatic ecological and socioeconomic consequences. However, our analyses indicate that the epipelagic response to La Niña events that typically follows extreme El Niño is far from a perfect mirror image of El Niño (Figure 4d-f), with the increase in biomass associated with extreme El Niño located in the central/eastern equatorial Pacific, while the decrease in biomass associated with the following La Niña remains confined to the western Pacific. These asymmetries associated with this ecosystem response also appear to be considerably larger than those associated with the physical response (Figure 4a) or the chlorophyll response (Figure 4c). A more refined assessment of the

asymmetries in the response of marine ecosystems to ENSO and their associated driving processes is outside the scope of this study but deserves to be explored in detail in the future.

Although the historical simulation from our ecosystem model compares favorably with observations, it nevertheless has a number of limitations that deserve discussion. First, the model configuration used here corresponds to the level of generality that has been used in FishMIP to date. It simulates a single generic community for epipelagic organisms and two mesopelagic communities. We thus did not implement any temperature limitation to be as generic as possible and do not take into account the specifics of tuna physiology. Since these specifics are likely to affect the results, configuring APECOSM to specifically represent tuna species would help to refine our findings for particular species. We were also surprised to find that the role of active movements is negligible compared to passive movements, even for large organisms. Since this result may suggest an underestimation of active transport in our simulation, it is important to estimate more precisely the value of the movement parameters used from tagging data for example, and to study the sensitivity of our results to the value of this parameter.

Among the future developments envisioned, our modelling framework allows for sensitivity experiments where the interannual variations in key environmental factors (temperature, currents, food) can be artificially frozen to separate their relative influence on the food web dynamics. We also plan to examine the ENSO-related response of mesopelagic communities that are also explicitely simulated by our model. Finally, we plan to extend our analysis to other regions subject to significant climate variations, such as the

Indian Ocean, which is home to the Indian Ocean Dipole (IOD), and to the analysis of climate change effects at the global scale. While the latter has been the focus of several recent studies (e.g. Lotze et al., 2019; Tittensor et al., 2021), and the factors responsible for the strongest climate impacts discussed (e.g. Heneghan et al., 2021), a finer mechanistic analysis of the bio-ecological processes that climate change would bring into play in global marine ecosystems has not yet been conducted.

Reliable estimations of the magnitude of the impact of climate change on marine ecosystems and associated ecosystem services requires reliable numerical projections. Significant progress has been made in terms of modeling marine ecosystems and using them to project the impact of possible future climate change and construct relevant ensemble analyses (e.g. Lotze et al., 2019; Tittensor et al., 2021). These analyses have notably contributed to the work of the IPCC (Pörtner et al., 2019, 2022) and IPBES (Brondizio et al., 2019) and it is important that the scientific community maintains this effort. However, the ability of the models used in these projections to reproduce the effects of past climate variability on ecosystems has not been thoroughly assessed yet, in particular due to the lack of relevant synoptic observations of high trophic levels. Yet, such an assessment is necessary and should be conducted to increase our confidence in these projections.

Finally, the magnitude of the expected climate change is such that marine ecosystems will operate in states without known analogues in the past. Mechanistic studies based on the fundamental principles governing the effects of past climate variability on marine ecosystems are very important in this regard. They help us to better understand the mechanisms that will be at

play in those future no-analogue situations, when projections based on statistical analysis may become invalid. This can only increase our confidence in the future response projected by integrated ecosystem models to climate change, and allow us to better understand their diversity.

Acknowledgement

The authors acknowledge the Pôle de Calcul et de Données Marines (PCDM, `http://www.ifremer.fr/pcdm`) for providing DATARMOR storage, data access, computational resources, visualization and support services. The APECOSM version used in this study is the 4.0.1. Data analysis and representation has been performed using Python 3.9.4. Covariance analysis and detrending has been performed using the *numpy* and *scipy* packages. Plots and maps have been made by using the *matplotlib* and *cartopy* packages. The tuna drawing in Figure 9 is courtesy of Tchiiweb (http://www.tchiiweb.com/). The Pacific data presented in this study and the scripts used in the analysis will be available on Zenodo (`https://doi.org/10.5281/zenodo.7142804`).

List of Figures

List of Tables

References

Allain, V., Pilling, G. M., Williams, P. G., Harley, S., Nicol, S., & Hampton, J. (2018). Overview of tuna fisheries, stock status and management framework in the Western and Central Pacific Ocean. In E. Fache, & S. Pauwels (Eds.), *Fisheries in the Pacific : The Challenges of Governance and Sustainability* Cahiers Du Credo (pp. 19–48). Marseille: pacific-credo Publications.

An, S.-I., Tziperman, E., Okumura, Y. M., & Li, T. (2020). ENSO Irregularity and Asymmetry. In *El Niño Southern Oscillation in a Changing Climate* chapter 7. (pp. 153–172). American Geophysical Union (AGU). doi:10.1002/9781119548164.ch7.

Aumont, O., Ethé, C., Tagliabue, A., Bopp, L., & Gehlen, M. (2015). PISCES-v2: An ocean biogeochemical model for carbon and ecosystem studies. *Geoscientific Model Development*, *8*, 2465–2513. doi:10.5194/gmd-8-2465-2015.

Barber, R. T., & Chavez, F. P. (1983). Biological Consequences of El Niño. *Science*, . doi:10.1126/science.222.4629.1203.

Batista, V. S., Fabré, N. N., Malhado, A. C. M., & Ladle, R. J. (2014). Tropical Artisanal Coastal Fisheries: Challenges and Future Directions. *Reviews in Fisheries Science & Aquaculture*, *22*, 1–15. doi:10.1080/10641262.2013.822463.

Bertrand, A., Josse, E., Bach, P., Gros, P., & Dagorn, L. (2002). Hydrological and trophic characteristics of tuna habitat: Consequences on tuna

distribution and longline catchability. *Canadian Journal of Fisheries and Aquatic Sciences*, *59*, 1002–1013. doi:10.1139/f02-073.

Bertrand, A., Lengaigne, M., Takahashi, K., Avadí, A., & Harrod, C. (2020). *El Niño Southern Oscillation (ENSO) Effects on Fisheries and Aquaculture*. Food & Agriculture Org.

Blanke, B., & Delecluse, P. (1993). Variability of the Tropical Atlantic Ocean Simulated by a General Circulation Model with Two Different Mixed-Layer Physics. *Journal of Physical Oceanography*, *23*, 1363–1388. doi:10.1175/1520-0485(1993)023<1363:VOTTAO>2.0.CO;2.

Bretherton, C. S., Widmann, M., Dymnikov, V. P., Wallace, J. M., & Bladé, I. (1999). The Effective Number of Spatial Degrees of Freedom of a Time-Varying Field. *Journal of Climate*, *12*, 1990–2009. doi:10.1175/1520-0442(1999)012<1990:TENOSD>2.0.CO;2.

Brondizio, E., Settele, J., Díaz, S., & Ngo, H. T. (2019). *Global Assessment Report on Biodiversity and Ecosystem Services of the Intergovernmental Science-Policy Platform on Biodiversity and Ecosystem Services.*. Technical Report IPBES (2019).

Cai, W., McPhaden, M. J., Grimm, A. M., Rodrigues, R. R., Taschetto, A. S., Garreaud, R. D., Dewitte, B., Poveda, G., Ham, Y.-G., Santoso, A., Ng, B., Anderson, W., Wang, G., Geng, T., Jo, H.-S., Marengo, J. A., Alves, L. M., Osman, M., Li, S., Wu, L., Karamperidou, C., Takahashi, K., & Vera, C. (2020). Climate impacts of the El Niño–Southern Oscillation

on South America. *Nature Reviews Earth & Environment*, *1*, 215–231. doi:10.1038/s43017-020-0040-3.

Cai, W., Santoso, A., Collins, M., Dewitte, B., Karamperidou, C., Kug, J.-S., Lengaigne, M., McPhaden, M. J., Stuecker, M. F., Taschetto, A. S., Timmermann, A., Wu, L., Yeh, S.-W., Wang, G., Ng, B., Jia, F., Yang, Y., Ying, J., Zheng, X.-T., Bayr, T., Brown, J. R., Capotondi, A., Cobb, K. M., Gan, B., Geng, T., Ham, Y.-G., Jin, F.-F., Jo, H.-S., Li, X., Lin, X., McGregor, S., Park, J.-H., Stein, K., Yang, K., Zhang, L., & Zhong, W. (2021). Changing El Niño–Southern Oscillation in a warming climate. *Nature Reviews Earth & Environment*, *2*, 628–644. doi:10.1038/s43017-021-00199-z.

Chavez, F. P., Strutton, P. G., Friederich, G. E., Feely, R. A., Feldman, G. C., Foley, D. G., & McPhaden, M. J. (1999). Biological and Chemical Response of the Equatorial Pacific Ocean to the 1997-98 El Niño. *Science*, *286*, 2126–2131. doi:10.1126/science.286.5447.2126.

Claar, D. C., Szostek, L., McDevitt-Irwin, J. M., Schanze, J. J., & Baum, J. K. (2018). Global patterns and impacts of El Niño events on coral reefs: A meta-analysis. *PLOS ONE*, *13*, e0190957. doi:10.1371/journal.pone.0190957.

Coulter, A., Cashion, T., Cisneros-Montemayor, A. M., Popov, S., Tsui, G., Le Manach, F., Schiller, L., Palomares, M. L. D., Zeller, D., & Pauly, D. (2020). Using harmonized historical catch data to infer the expansion of global tuna fisheries. *Fisheries Research*, *221*, 105379. doi:10.1016/j.fishres.2019.105379.

Drushka, K., Bellenger, H., Guilyardi, E., Lengaigne, M., Vialard, J., & Madec, G. (2015). Processes driving intraseasonal displacements of the eastern edge of the warm pool: The contribution of westerly wind events. *Climate Dynamics*, *44*, 735–755. doi:10.1007/s00382-014-2297-z.

Eakin, C. M., Sweatman, H. P. A., & Brainard, R. E. (2019). The 2014–2017 global-scale coral bleaching event: Insights and impacts. *Coral Reefs*, *38*, 539–545. doi:10.1007/s00338-019-01844-2.

FAO (2022). *The State of World Fisheries and Aquaculture 2022: Towards Blue Transformation*. Number 2022 in The State of World Fisheries and Aquaculture (SOFIA). Rome, Italy: FAO. doi:10.4060/cc0461en.

Faugeras, B., & Maury, O. (2005). An advection-diffusion-reaction size-structured fish population dynamics model combined with a statistical parameter estimation procedure: Application to the Indian Ocean skipjack tuna fishery. *Mathematical Biosciences and Engineering*, *2*, 719. doi:10.3934/mbe.2005.2.719.

Fonteneau, A. (1998). *Atlas of Tropical Tuna Fisheries. World Catches and Environment*. IRD Orstom.

Forsythe, W. C., Rykiel, E. J., Stahl, R. S., Wu, H.-i., & Schoolfield, R. M. (1995). A model comparison for daylength as a function of latitude and day of year. *Ecological Modelling*, *80*, 87–95. doi:10.1016/0304-3800(94)00034-F.

Glynn, P. W. (1988). EL NIÑO-SOUTHERN OSCILLATION 1982-1983:

NEARSHORE POPULATION, COMMUNITY, AND ECOSYSTEM RESPONSES. *Annual Review of Ecology and Systematics*, *19*, 309–346.

Glynn, P. W., Maté, J. L., Baker, A. C., & Calderón, M. O. (2001). Coral bleaching and mortality in Panama and Ecuador during the 1997-1998 El Niño-Southern Oscillation event: Spatial/temporal patterns and comparisons with the 1982-1983 event. *Bulletin of Marine Science*, *69*, 79–109.

Gorgues, T., Menkes, C., Slemons, L., Aumont, O., Dandonneau, Y., Radenac, M. H., Alvain, S., & Moulin, C. (2010). Revisiting the La Niña 1998 phytoplankton blooms in the equatorial Pacific. *Deep Sea Research Part I: Oceanographic Research Papers*, *57*, 567–576. doi:10.1016/j.dsr.2009.12.008.

Guiet, J., Bianchi, D., Maury, O., Barrier, N., & Kessouri, F. (2022). Movement Shapes the Structure of Fish Communities Along a Cross-Shore Section in the California Current. *Frontiers in Marine Science*, *9*.

Heneghan, R. F., Galbraith, E., Blanchard, J. L., Harrison, C., Barrier, N., Bulman, C., Cheung, W., Coll, M., Eddy, T. D., Erauskin-Extramiana, M., Everett, J. D., Fernandes-Salvador, J. A., Gascuel, D., Guiet, J., Maury, O., Palacios-Abrantes, J., Petrik, C. M., du Pontavice, H., Richardson, A. J., Steenbeek, J., Tai, T. C., Volkholz, J., Woodworth-Jefcoats, P. A., & Tittensor, D. P. (2021). Disentangling diverse responses to climate change among global marine ecosystem models. *Progress in Oceanography*, *198*, 102659. doi:10.1016/j.pocean.2021.102659.

Hobday, A. J., & Evans, K. (2013). Detecting climate impacts with oceanic

fish and fisheries data. *Climatic Change*, *119*, 49–62. doi:10.1007/s10584-013-0716-5.

Holbrook, N. J., Sen Gupta, A., Oliver, E. C. J., Hobday, A. J., Benthuysen, J. A., Scannell, H. A., Smale, D. A., & Wernberg, T. (2020). Keeping pace with marine heatwaves. *Nature Reviews Earth & Environment*, *1*, 482–493. doi:10.1038/s43017-020-0068-4.

IOC, SCOR, & IAPSO (2010). *The International Thermodynamic Equation of Seawater - 2010: Calculation and Use of Thermodynamic Properties*. Technical Report Intergovernmental Oceanographic Commission.

Kim, E., Moon, D., & Kim, S. (2015). Effects of Climate-induced Variation in the Catch Distribution and Biological Characteristics of Skipjack Tuna Katsuwonus pelamis in the Western and Central Pacific Ocean -Korean Journal of Fisheries and Aquatic Sciences — Korea Science. *Korean Journal of Fisheries and Aquatic Sciences*, *48*, 489–497.

Kobayashi, S., Ota, Y., Harada, Y., Ebita, A., Moriya, M., Onoda, H., Onogi, K., Kamahori, H., Kobayashi, C., Endo, H., Miyaoka, K., & Takahashi, K. (2015). The JRA-55 Reanalysis: General Specifications and Basic Characteristics. *Journal of the Meteorological Society of Japan. Ser. II*, *93*, 5–48. doi:10.2151/jmsj.2015-001.

Koojman, S. (2010). *Dynamic Energy Budget Theory for Metabolic Organisation*. (3rd ed.).

Le Mézo, P., Lefort, S., Séférian, R., Aumont, O., Maury, O., Murtugudde, R., & Bopp, L. (2016). Natural variability of marine ecosystems inferred

from a coupled climate to ecosystem simulation. *Journal of Marine Systems*, *153*, 55–66. doi:10.1016/j.jmarsys.2015.09.004.

Lehodey, P. (2001). The pelagic ecosystem of the tropical Pacific Ocean: Dynamic spatial modelling and biological consequences of ENSO. *Progress in Oceanography*, *49*, 439–468. doi:10.1016/S0079-6611(01)00035-0.

Lehodey, P., Bertignac, M., Hampton, J., Lewis, A., & Picaut, J. (1997). El Niño Southern Oscillation and tuna in the western Pacific. *Nature*, *389*, 715–718. doi:10.1038/39575.

Lehodey, P., Bertrand, A., Hobday, A. J., Kiyofuji, H., McClatchie, S., Menkès, C. E., Pilling, G., Polovina, J., & Tommasi, D. (2020). ENSO Impact on Marine Fisheries and Ecosystems. In *El Niño Southern Oscillation in a Changing Climate* chapter 19. (pp. 429–451). American Geophysical Union (AGU). doi:10.1002/9781119548164.ch19.

Lehodey, P., Senina, I., & Murtugudde, R. (2008). A spatial ecosystem and populations dynamics model (SEAPODYM) – Modeling of tuna and tuna-like populations. *Progress in Oceanography*, *78*, 304–318. doi:10.1016/j.pocean.2008.06.004.

Lengaigne, M., Boulanger, J.-P., Menkes, C., Masson, S., Madec, G., & Delecluse, P. (2002). Ocean response to the March 1997 Westerly Wind Event. *Journal of Geophysical Research: Oceans*, *107*, SRF 16–1–SRF 16–20. doi:10.1029/2001JC000841.

Lengaigne, M., Hausmann, U., Madec, G., Menkes, C., Vialard, J., & Molines, J. M. (2012). Mechanisms controlling warm water volume interannual

variations in the equatorial Pacific: Diabatic versus adiabatic processes. *Climate Dynamics*, *38*, 1031–1046. doi:10.1007/s00382-011-1051-z.

Lengaigne, M., Madec, G., Menkes, C., & Alory, G. (2003). Impact of isopycnal mixing on the tropical ocean circulation. *Journal of Geophysical Research: Oceans*, *108*. doi:10.1029/2002JC001704.

Leung, S., Thompson, L., McPhaden, M. J., & Mislan, K. A. S. (2019). ENSO drives near-surface oxygen and vertical habitat variability in the tropical Pacific. *Environmental Research Letters*, *14*, 064020. doi:10.1088/1748-9326/ab1c13.

Levier, B., Tréguier, A.-M., Madec, G., & Garnier, V. (2007). Free surface and variable volume in the NEMO code.

Lodge, M. W. (1998). The development of the Palau Arrangement for the management of the Western Pacific Purse Seine Fishery. *Marine Policy*, *22*, 1–28. doi:10.1016/S0308-597X(97)00024-9.

Lotze, H. K., Tittensor, D. P., Bryndum-Buchholz, A., Eddy, T. D., Cheung, W. W. L., Galbraith, E. D., Barange, M., Barrier, N., Bianchi, D., Blanchard, J. L., Bopp, L., Büchner, M., Bulman, C. M., Carozza, D. A., Christensen, V., Coll, M., Dunne, J. P., Fulton, E. A., Jennings, S., Jones, M. C., Mackinson, S., Maury, O., Niiranen, S., Oliveros-Ramos, R., Roy, T., Fernandes, J. A., Schewe, J., Shin, Y.-J., Silva, T. A. M., Steenbeek, J., Stock, C. A., Verley, P., Volkholz, J., Walker, N. D., & Worm, B. (2019). Global ensemble projections reveal trophic amplification of ocean biomass

declines with climate change. *Proceedings of the National Academy of Sciences*, *116*, 12907–12912. doi:10.1073/pnas.1900194116.

Madec, G., Bourdallé-Badie, R., Chanut, J., Clementi, E., Coward, A., Ethé, C., Iovino, D., Lea, D., Lévy, C., Lovato, T., Martin, N., Masson, S., Mocavero, S., Rousset, C., Storkey, D., Vancoppenolle, M., Müeller, S., Nurser, G., Bell, M., & Samson, G. (2019). *NEMO Ocean Engine*. Technical Report IPSL. doi:10.5281/zenodo.1464816.

Madec, G., & Imbard, M. (1996). A global ocean mesh to overcome the North Pole singularity. *Climate Dynamics*, *12*, 381–388. doi:10.1007/BF00211684.

Martinez, E., Gorgues, T., Lengaigne, M., Fontana, C., Sauzède, R., Menkes, C., Uitz, J., Di Lorenzo, E., & Fablet, R. (2020). Reconstructing Global Chlorophyll-a Variations Using a Non-linear Statistical Approach. *Frontiers in Marine Science*, *7*.

Masotti, I., Moulin, C., Alvain, S., Bopp, L., Tagliabue, A., & Antoine, D. (2011). Large-scale shifts in phytoplankton groups in the Equatorial Pacific during ENSO cycles. *Biogeosciences*, *8*, 539–550. doi:10.5194/bg-8-539-2011.

Maury, O. (2010). An overview of APECOSM, a spatialized mass balanced "Apex Predators ECOSystem Model" to study physiologically structured tuna population dynamics in their ecosystem. *Progress in Oceanography*, *84*, 113–117. doi:10.1016/j.pocean.2009.09.013.

Maury, O. (2017). Can schooling regulate marine populations and ecosystems? *Progress in Oceanography*, *156*, 91–103. doi:10.1016/j.pocean.2017.06.003.

Maury, O., & Poggiale, J.-C. (2013). From individuals to populations to communities: A dynamic energy budget model of marine ecosystem size-spectrum including life history diversity. *Journal of Theoretical Biology*, *324*, 52–71. doi:10.1016/j.jtbi.2013.01.018.

Maury, O., Shin, Y.-J., Faugeras, B., Ben Ari, T., & Marsac, F. (2007). Modeling environmental effects on the size-structured energy flow through marine ecosystems. Part 2: Simulations. *Progress in Oceanography*, *74*, 500–514. doi:10.1016/j.pocean.2007.05.001.

Murtugudde, R. G., Signorini, S. R., Christian, J. R., Busalacchi, A. J., McClain, C. R., & Picaut, J. (1999). Ocean color variability of the tropical Indo-Pacific basin observed by SeaWiFS during 1997–1998. *Journal of Geophysical Research: Oceans*, *104*, 18351–18366. doi:10.1029/1999JC900135.

Paulson, C. A., & Simpson, J. J. (1977). Irradiance Measurements in the Upper Ocean. *Journal of Physical Oceanography*, *7*, 952–956. doi:10.1175/1520-0485(1977)007<0952:IMITUO>2.0.CO;2.

Philander, S. G. H., & Seigel, A. D. (1985). Chapter 33 Simulation of El Niño of 1982–1983. In J. C. J. Nihoul (Ed.), *Elsevier Oceanography Series* (pp. 517–541). Elsevier volume 40 of *Coupled Ocean-Atmosphere Models*. doi:10.1016/S0422-9894(08)70729-3.

Picaut, J., Ioualalen, M., Delcroix, T., Masia, F., Murtugudde, R., & Vialard, J. (2001). The oceanic zone of convergence on the eastern edge of the Pacific warm pool: A synthesis of results and implications for El Niño-Southern Oscillation and biogeochemical phenomena. *Journal of Geophysical Research: Oceans*, *106*, 2363–2386. doi:10.1029/2000JC900141.

Pörtner, H.-O., Roberts, D. C., Masson-Delmotte, V., Zhai, P., Tignor, M., Poloczanska, E., Mintenbeck, K., Alegría, A., Nicolai, M., Okem, A., Petzold, J., Rama, B., & Weyer, N. M. (2019). *IPCC Special Report on the Ocean and Cryosphere in a Changing Climate*. Technical Report IPCC (2019).

Pörtner, H.-O., Roberts, D. C., Tignor, M., Poloczanska, E. S., Mintenbeck, K., Alegría, A., Craig, M., Langsdorf, S., Löschke, S., Möller, V., Okem, A., & Rama, B. (2022). *Climate Change 2022: Impacts, Adaptation, and Vulnerability. Contribution of Working Group II to the Sixth Assessment Report of the Intergovernmental Panel on Climate Change*. Technical Report IPCC (2022).

Puy, M., Vialard, J., Lengaigne, M., Guilyardi, E., Voldoire, A., & Madec, G. (2019). Modulation of equatorial Pacific sea surface temperature response to westerly wind events by the oceanic background state. *Climate Dynamics*, *52*, 7267–7291. doi:10.1007/s00382-016-3480-1.

Rayner, N. A., Parker, D. E., Horton, E. B., Folland, C. K., Alexander, L. V., Rowell, D. P., Kent, E. C., & Kaplan, A. (2003). Global analyses of sea surface temperature, sea ice, and night marine air temperature since the

late nineteenth century. *Journal of Geophysical Research: Atmospheres*, *108*. doi:10.1029/2002JD002670.

Rio, M.-H., Mulet, S., & Picot, N. (2014). Beyond GOCE for the ocean circulation estimate: Synergetic use of altimetry, gravimetry, and in situ data provides new insight into geostrophic and Ekman currents. *Geophysical Research Letters*, *41*, 8918–8925. doi:10.1002/2014GL061773.

Santoso, A., Mcphaden, M. J., & Cai, W. (2017). The Defining Characteristics of ENSO Extremes and the Strong 2015/2016 El Niño. *Reviews of Geophysics*, *55*, 1079–1129. doi:10.1002/2017RG000560.

Sathyendranath, S., Brewin, R. J. W., Brockmann, C., Brotas, V., Calton, B., Chuprin, A., Cipollini, P., Couto, A. B., Dingle, J., Doerffer, R., Donlon, C., Dowell, M., Farman, A., Grant, M., Groom, S., Horseman, A., Jackson, T., Krasemann, H., Lavender, S., Martinez-Vicente, V., Mazeran, C., Mélin, F., Moore, T. S., Müller, D., Regner, P., Roy, S., Steele, C. J., Steinmetz, F., Swinton, J., Taberner, M., Thompson, A., Valente, A., Zühlke, M., Brando, V. E., Feng, H., Feldman, G., Franz, B. A., Frouin, R., Gould, R. W., Hooker, S. B., Kahru, M., Kratzer, S., Mitchell, B. G., Muller-Karger, F. E., Sosik, H. M., Voss, K. J., Werdell, J., & Platt, T. (2019). An Ocean-Colour Time Series for Use in Climate Studies: The Experience of the Ocean-Colour Climate Change Initiative (OC-CCI). *Sensors*, *19*, 4285. doi:10.3390/s19194285.

Schaefer, K. M., & Fuller, D. W. (2002). Movements, behavior, and habitat selection of bigeye tuna (Thunnus obesus) in the eastern equatorial Pacific,

ascertained through archival tags — Scientific Publications Office. *Fishery Bulletin*, (pp. 765–788).

Senina, I., Sibert, J., & Lehodey, P. (2008). Parameter estimation for basin-scale ecosystem-linked population models of large pelagic predators: Application to skipjack tuna. *Progress in Oceanography*, *78*, 319–335. doi:10.1016/j.pocean.2008.06.003.

Stramma, L., Fischer, T., Grundle, D. S., Krahmann, G., Bange, H. W., & Marandino, C. A. (2016). Observed El Niño conditions in the eastern tropical Pacific in October 2015. *Ocean Science*, *12*, 861–873. doi:10.5194/os-12-861-2016.

Taconet, P., Chassot, E., & Barde, J. (2018). Global monthly catch of tuna, tuna-like and shark species (1950-2015) aggregated by 1° or 5° squares (IRD level 2).

Takahashi, K., Montecinos, A., Goubanova, K., & Dewitte, B. (2011). ENSO regimes: Reinterpreting the canonical and Modoki El Niño. *Geophysical Research Letters*, *38*. doi:10.1029/2011GL047364.

Tickler, D., Meeuwig, J. J., Palomares, M.-L., Pauly, D., & Zeller, D. (2018). Far from home: Distance patterns of global fishing fleets. *Science Advances*, *4*, eaar3279. doi:10.1126/sciadv.aar3279.

Tittensor, D. P., Eddy, T. D., Lotze, H. K., Galbraith, E. D., Cheung, W., Barange, M., Blanchard, J. L., Bopp, L., Bryndum-Buchholz, A., Büchner, M., Bulman, C., Carozza, D. A., Christensen, V., Coll, M., Dunne, J. P., Fernandes, J. A., Fulton, E. A., Hobday, A. J., Huber, V., Jennings, S.,

Jones, M., Lehodey, P., Link, J. S., Mackinson, S., Maury, O., Niiranen, S., Oliveros-Ramos, R., Roy, T., Schewe, J., Shin, Y.-J., Silva, T., Stock, C. A., Steenbeek, J., Underwood, P. J., Volkholz, J., Watson, J. R., & Walker, N. D. (2018). A protocol for the intercomparison of marine fishery and ecosystem models: Fish-MIP v1.0. *Geoscientific Model Development*, *11*, 1421–1442. doi:10.5194/gmd-11-1421-2018.

Tittensor, D. P., Novaglio, C., Harrison, C. S., Heneghan, R. F., Barrier, N., Bianchi, D., Bopp, L., Bryndum-Buchholz, A., Britten, G. L., Büchner, M., Cheung, W. W. L., Christensen, V., Coll, M., Dunne, J. P., Eddy, T. D., Everett, J. D., Fernandes-Salvador, J. A., Fulton, E. A., Galbraith, E. D., Gascuel, D., Guiet, J., John, J. G., Link, J. S., Lotze, H. K., Maury, O., Ortega-Cisneros, K., Palacios-Abrantes, J., Petrik, C. M., du Pontavice, H., Rault, J., Richardson, A. J., Shannon, L., Shin, Y.-J., Steenbeek, J., Stock, C. A., & Blanchard, J. L. (2021). Next-generation ensemble projections reveal higher climate risks for marine ecosystems. *Nature Climate Change*, *11*, 973–981. doi:10.1038/s41558-021-01173-9.

Valle, C. A., Cruz, F., Cruz, J. B., Merlen, G., & Coulter, M. C. (1987). The impact of the 1982–1983 El Niño-Southern Oscillation on seabirds in the Galapagos Islands, Ecuador. *Journal of Geophysical Research: Oceans*, *92*, 14437–14444. doi:10.1029/JC092iC13p14437.

Vialard, J., Menkes, C., Boulanger, J.-P., Delecluse, P., Guilyardi, E., McPhaden, M. J., & Madec, G. (2001). A Model Study of Oceanic Mechanisms Affecting Equatorial Pacific Sea Surface Temperature during

the 1997–98 El Niño. *Journal of Physical Oceanography*, *31*, 1649–1675. doi:10.1175/1520-0485(2001)031<1649:AMSOOM>2.0.CO;2.

Williams, & Terawasi (2014). Overview of Tuna Fisheries in the Western and Central Pacific Ocean, Including Economic Conditions.

Williams, P., & Ruaia, T. (2021). *Overview of Tuna Fisheries in the Western and Central Pacific Ocean, Including Economic Conditions – 2021*. Technical Report Western and Central Pacific Fisheries Commission.

Yen, K.-W., & Lu, H.-J. (2016). Spatial–temporal variations in primary productivity and population dynamics of skipjack tuna Katsuwonus pelamis in the western and central Pacific Ocean. *Fisheries Science*, *82*, 563–571. doi:10.1007/s12562-016-0992-x.

Declaration of interests

☒ The authors declare that they have no known competing financial interests or personal relationships that could have appeared to influence the work reported in this paper.

☐ The authors declare the following financial interests/personal relationships which may be considered as potential competing interests: